Formation of Zn- and O- vacancy clusters in ZnO through deuterium annealing

K. M. Johansen,[1] F. Tuomisto,[2] I. Makkonen,[2] and L. Vines[1]

[1] *University of Oslo, Centre for Materials Science and Nanotechnology, 0318 Oslo, Norway*
[2] *Department of Applied Physics, Aalto University, P.O. Box 15100, 00076 Aalto, Espoo, Finland*

(Dated: July 25, 2016)

Open volume defects, clearly distinguishable from the isolated Zn-vacancy are observed in hydrothermally grown ZnO after exposure to deuterium gas at elevated temperatures. From a combination of secondary ion mass spectrometry (SIMS), positron annihilation spectroscopy (PAS) and density functional theory (DFT) calculations it is found that as a result of this treatment vacancy clusters consisting of minimum one Zn- and one O-vacancy are formed, in contrast to introduction of isolated O-vacancies. A scenario for the cluster formation is proposed, where Zn- and O-vacancies originate from the bulk of the sample and the sample surface, respectively. A fraction of the vacancy clusters are decorated by Li and/or H and may therefore be indirectly observed by SIMS. The peak in Li-concentration at about 100 nm below the sample surface, as observed by SIMS is in good correspondence with the PAS-results.

I. INTRODUCTION

Intrinsic defects in ZnO have attracted substantial research interest, due to their direct impact on the electrical properties of the material. Controlling the different intrinsic defects is therefore the key to utilizing ZnO in a vast range of applications. Among the most studied intrinsic defects are the oxygen- (V_O) and zinc-vacancies (V_{Zn}). The formation energies of V_O and V_{Zn} are predicted to be lower than those of their interstitial counterparts, zinc interstitial (Zn_i) and oxygen interstitial (O_i).[1, 2]. Hence, when the material is exposed to Zn-rich and/or reducing conditions, V_O will dominate in concentration as compared to Zn_i. In contrast to these predictions V_O is typically not observed in ZnO exposed to different thermal treatments, but frequently appears in samples that have been exposed to conditions far from its thermodynamical equilibrium, e.g., through electron irradiation experiments[3]. In electron irradiated samples the V_O has been identified using electron paramagnetic resonance (EPR) spectroscopy (g-value ∼1.99)[4–7]. V_{Zn}, on the other hand, is typically observed in as-grown material and found to be the dominating compensating acceptor in n-type ZnO.[8] Its behavior has been studied, e.g,. by positron annihilation spectroscopy (PAS), a technique especially sensitive to negatively charged open volume defects.[9]

Although V_O and V_{Zn} have been extensively studied, less is known about larger vacancy clusters. There are several observations from PAS of open volume defects different from the V_{Zn} and with a larger open volume emerging in samples implanted with various elements, e.g., H, N and Al, were the defect is argued to consist of clusters of vacancies[10–14] In a similar study, Chan et al.[15] directly observed the formation of microvoids in cross sectional transmission electron microscopy images on samples implanted with $1\times10^{17}\text{cm}^{-2}$ H at 100 keV and exposed to post implantation annealing at 600 °C.

In a study by Chen et al. samples exposed to a dose of $5.5\times10^{18}\text{cm}^{-2}$ 3 MeV electrons followed by post irradiation annealing, two different defects was observed; One was identified as the isolated V_{Zn}, while the other was tentatively identified as a $V_{Zn}V_O$-complex. Recently, such a di-vacancy complex consisting of V_{Zn} and V_O was identified in neutron irradiated ZnO samples using EPR, directly confirming their existence.[16] Furthermore, Makkonen et al. [17] predicted from density functional theory calculations that vacancy clusters formed by different numbers of V_{Zn} and V_O can be observed by and to a certain extent distinguished by PAS.

In this study, we report on the observation of open volume defects larger than the isolated V_{Zn}, formed by heat treatment in deuterium gas (D_2). These clusters are suggested to form due to in-diffusion of V_O from the surface followed by a defect reaction with V_{Zn}, initially present in the as-grown material, and effectively trapping both V_O and V_{Zn} into a stable cluster, thereby preventing the introduction of isolated V_O and resulting in a redistribution of V_{Zn}. Such a vacancy clustering may also explain the discrepancy between the predicted formation of isolated V_O and the lack of experimental observation of V_O in samples exposed to reducing and/or Zn-rich conditions during heat treatment.

II. METHODOLOGY

Five samples originating from two similar wafers of n-type HT-ZnO supplied by SPC-Goodwill were used in this study. One sample was kept as an as-grown reference sample (labeled AsG). Three samples were heat treated in a closed quartz ampule filled with 0.5 Bar of wet (D_2O) (D_2)-gas at 600 °C, 650 °C and 700 °C labeled D-600, D-650 and D-700, respectively. The final piece was heat treated at 1500 °C for 1 h, followed by polishing of the O-face and subsequent heat treatment at 1100 °C for 1 h to remove defects induced by polishing (labeled LowLi).[18] The samples AsG and LowLi can be viewed as reference samples with and without Li.

D and Li concentration profiles were obtained by secondary ion mass spectrometry (SIMS), using a Cameca

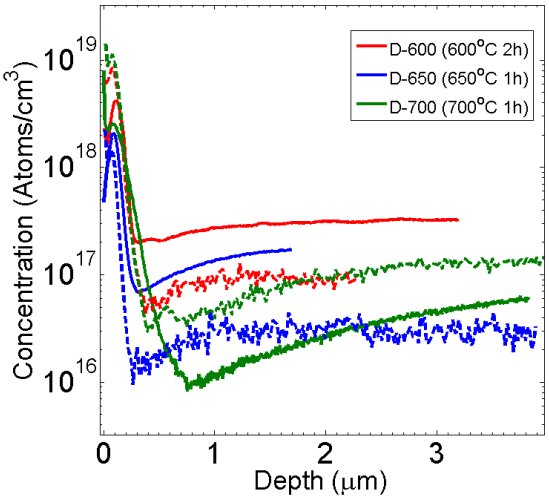

FIG. 1. D- (dashed lines) and Li- (solid lines) concentration measured by SIMS after hydrogenation in an ampule filled with 0.5 bar D_2-gas in the range of $600-700\,^{\circ}$C.

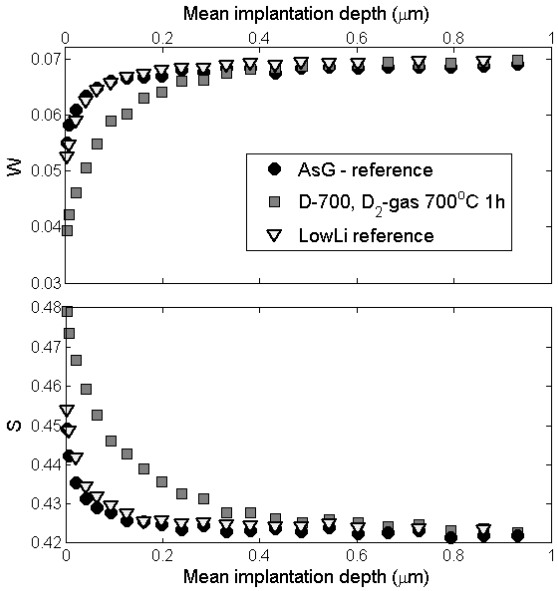

FIG. 2. Absolute W- and S-parameter measured in the as-grown B-1, the hydrogenated B-2 and the Li-lean B-3 samples. The increased (decreased) signal close to the surface as seen for S(W) in sample B-1 and B-3 is due to surface annihilation. The signal observed in B-1 is a result of both surface annihilation and annihilation in sub surface positron traps.

IMS7f microanalyzer. The concentration calibration was performed using implanted reference samples, which results in an uncertainty in the concentration values of less than 10%. A concentration of $2\times10^{17}\,\mathrm{Li/cm^3}$ was found in the as-grown (AsG) sample.

For the Doppler broadening experiments monoenergetic positrons were implanted into the ZnO samples at room temperature. The implantation energy of the positrons was varied in the range of 0.5−38 keV, giving a mean positron implantation depth of 0.05−2.4 μm. The Doppler broadening of the annihilation radiation was detected by two high-purity Ge detectors with an energy resolution of 1.24 keV at 511 keV. The data were analyzed using the conventional S- and W-parameters, defined as the fractions of counts in the central S, $|E-511\,\mathrm{keV}| \leq 0.8\,\mathrm{keV}$ (corresponding to electron momentum of ¡0.4 a.u.), and the wing W, $2.9\,\mathrm{keV} \leq |E-511\,\mathrm{keV}| \leq 7.4\,\mathrm{keV}$ (1.6 - 4.0 a.u.), parts of the recorded photon spectrum.

S and W parameters for different defect configurations have been calculated based on density functional theory (DFT) in the local density approximation (LDA) [19] as implemented in VASP[20, 21] and models for predicting positron states and annihilation in defects in solids. Technical details of the formalism to calculate the PAS-parameters can be found in Ref.25, and the supercell and technical details of the ZnO defect calculations are the same as used in Ref. 17. This approach is well-established and has been proven successful in various PAS studies[9].

III. RESULTS

Figure 1 shows the D and Li concentration profiles obtained by SIMS-measurements for the samples D-600, D-650 and D-700, which all were exposed to deuterium in a closed ampule while heat treated at temperatures in the range from $600-700\,^{\circ}$C. The SIMS results show a substantial accumulation of both D and Li about 100 nm below the sample surface. The Li peak concentration is in the range of $(2\text{-}4)\times10^{18}\,\mathrm{cm^{-3}}$. Furthermore, for sample D-650 and D-700 a notable reduction of the Li-concentration in the range between 0.5 and 1μm is followed by an increase in the Li-concentration as a function of increasing depth. For D the peak concentration reaches $\sim1\times10^{19}\,\mathrm{cm^{-3}}$ in the D-600 and D-700 samples, while in the D-650 sample it is about one order of magnitude lower ($1\times10^{18}\,\mathrm{cm^{-3}}$).

Figure 2 shows the absolute W and S- parameters plotted as a function of mean positron implantation depth for the AsG and hydrogenated sample D-700 together with the Li-lean reference sample, LowLi. The increase (decrease) in the signal observed from the surface down to a depth of approximately 100 nm for the W(S) parameter in the as-grown (B-1) and Li-lean (B-3) sample originates from positrons that diffuse towards the sample surface and annihilate there. An apparently similar behaviour of the data is observed for the S- and W-parameters in the D-700 sample, but it extends deeper (about 300 nm)

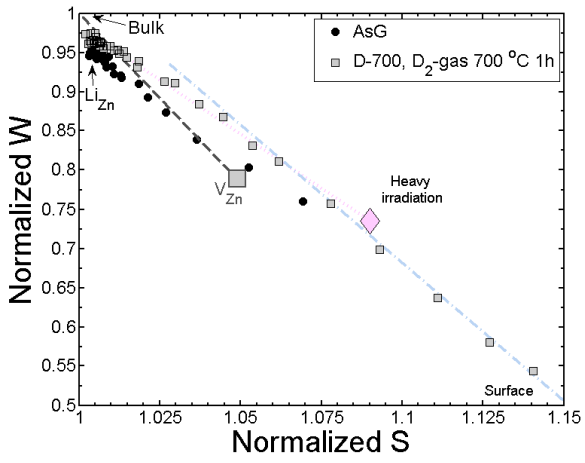

FIG. 3. The W- parameter is plotted as a function of the S-parameter as observed in the as-grown B-1 and the hydrogenated B-2 samples. The data are shown as normalized to the S and W parameters of a sample giving the parameters of the ZnO lattice[8]. The dashed line is referred to as the V_{Zn} - line, running between the bulk- and the saturated V_{Zn} annihilation parameters. [8, 9] In addition, the result of heavy O_2^{-1}-irradiation (W = 0.735 and S =1.09) is plotted[12, 27] and the dotted line is added as a guide to the eye. Furthermore, a dash-dot line is also added as a guide to show the influence of the surface annihilation on the experimental data.

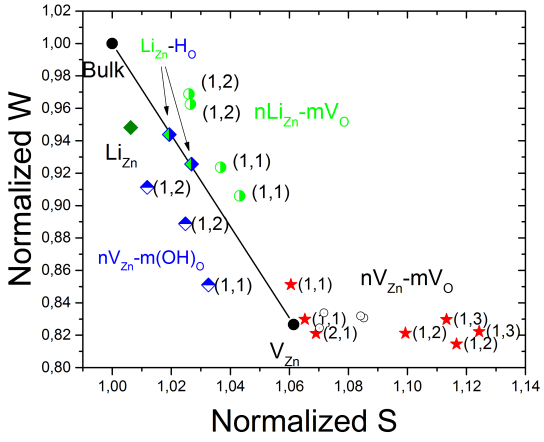

FIG. 4. W- and S-parameter annihilation parameters estimate based on DFT. The two black circles represent bulk and V_{Zn}, respectively. The red stars represents mV_{Zn}-nV_O clusters where m and n are integers given as (n,m) for the different configurations. The green diamond represent Li_{Zn}, green and blue diamonds $Li_{Zn}H_O$, and green circles Li_{Zn}-nV_O clusters.

with a higher amplitude as compared to the AsG and LowLi samples. This effect overlaps in depth with the large accumulation of D and Li as observed by SIMS.

H and D atoms are relatively mobile in ZnO with limited solubility[28, 29], but can readily be trapped and form more stable defect complexes. They only occur in the positive charge state[30], and are known to passivate acceptor type defects.[2, 31–34]. Thus H and D can be used as probes for defects in a similar manner as has been shown for Li[35, 36]. Hence, the accumulation of impurities below the sample surface is most likely explained by the presence of defects. Furthermore, judging from the variation in peak concentration of Li and D in the samples D-600, D-650 and D-700 (Fig. 1) the accumulation is limited by the number of D and Li atoms available to decorate the defects and not by the underlying defect concentration, which is not visible in the SIMS-measurements. Furthermore, a trap for hydrogen is also expected to trap positrons, since both H and positrons will be trapped by acceptor type defects. In view of this, it can be concluded that the increased value of the S and W parameters observed in Fig. 2 for the hydrogenated sample (D-700) originate from annihilation in open volume defects situated below the sample surface.

In order to identify this defect, figure 3 shows the W-parameter as a function of the S-parameter for the as-grown (AsG) and the hydrogenated (D-700) samples. In addition, previously reported parameters for saturated annihilation at the V_{Zn} (W = 0.79 and S = 1.049)[8, 9], the result after heavy O_2^{-1}-irradiation (W = 0.735 and S =1.09)[27] and a guide to the eye (dash-dot line) showing the influence of the surface annihilation is plotted for reference in figure. 3. For both the AsG- and D-700-samples the five data-points with the highest S-values correspond to positrons implanted with a mean implantation depth of less than 100 nm, where a significant amount of positrons diffuse towards and annihilate at the surface.

In the AsG-sample most of the data-points are concentrated around the position previously identified as the annihilation parameters for Li_{Zn} [37] and also stretching towards the V_{Zn} saturation trapping parameters and the surface annihilation state. For the D-700 sample, two differences are evident: (i) the data-points corresponding to the deepest mean implantation depth have shifted slightly towards the bulk parameters as compared to the data-points obtained for the as-grown sample (AsG). This shift reflects the lower Li_{Zn}-concentration in the bulk of the hydrogenated sample, see figure 1. Alternatively, this shift could be explained by a passivation of Li_{Zn} by deuterium as seen in Ref. 32. However, in this case the annihilation parameters should have shifted towards the V_{Zn}-line and not the ZnO-bulk value. (ii) the data-points are located to the right of the V_{Zn}-line, i.e., with a contribution to the annihilation parameters (W and S) originating from a defect with larger open volume than isolated V_{Zn}, thus excluding isolated V_{Zn}s as a candidate for the observed open volume defects.

Another open volume point defect to consider is V_O. Hydrogen gas is well known to lead to decomposition of ZnO, a process that is commonly utilized for vapor phase growth.[38] This behavior may, e.g., be explained in view of formation energies of the involved defects, which are predicted to increase from V_O, to interstitial H (H_i) and even higher for Zn_i.[2] In other words, V_O is the defect most likely to form while the Zn_i is the defect least likely to form. Hence, when ZnO is exposed to D_2-gas at elevated temperatures, there are in general two possibilities, (i) the gas will react with ZnO to form D_2O and O-poor ZnO and/or (ii) D will be dissolved in ZnO, e.g., forming interstitial D (D_i). For (i) both V_O and Zn_i may result from such a reaction, however, the large difference in formation energy between these two defects (in the order of 2-3 eV[2, 39]) will strongly promote the formation of V_O and lead to only minute concentrations of Zn_i. Furthermore, since D_i has a higher formation energy than V_O, it can be assumed that V_O will be more efficiently introduced as compared to D_i. Thereby making V_O a prime candidate to take part in the observed open volume defect. Room temperature Doppler Broadning experiments are, however, not sensitive to isolated V_O, which therefore excludes this possibility and leads us to consider the formation of vacancy-clusters. Interestingly, the formation of such a cluster can be viewed as the first step of ZnO decomposition.

As argued above, V_O is introduced at the surface, while V_{Zn} is typically observed to exist in the as-grown material, either as isolated V_{Zn} or filled with Li (Li_{Zn}).[37] From figure 3 it can be seen that the WS-plot is dominated by Li_{Zn} confirming the presence of Li_{Zn} in the as-grown sample. Furthermore, the minute concentration of Zn_i, will not be enough to remove the V_{Zn} from the sample. When heating to 700 °C for 2 h it can be estimated (assuming first order dissociation kinetics and an activation energy of 3.57 eV[40]) that more than 2% of the Li will be dissociated from the Zn-site into the Li_i. Li_i is highly mobile at these temperatures[41], however, as the sample is cooled down, Li_i will be trapped at, and thereby decorate, any available defect, e.g., V_{Zn}. From figure 1, it can be seen that a substantial amount of Li accumulate at the sample surface, and in addition both Li and D are observed to accumulate in the region of the open volume defects in the hydrogenated sample D-700. As a side-note, it should be mentioned that the accumulation of D is an important result since this type of treatment is a commonly used method to introduce H or D in ZnO, where the H or D concentration is typically assumed to be uniformly distributed within the material.[42–44] From first principle calculations the V_{Zn} migration barrier is estimated to be about 1 eV.[45, 46] Thus V_{Zn} is also expected to be mobile at these temperatures and may redistribute. In fact, the Li gradient observed from a depth of 0.8 μm and deeper combined with the accumulation of Li and D peaking at 100 nm, shows that V_{Zn} has diffused towards the sample surface due the presence of a V_{Zn}-sink/trap. V_O diffusing in from the sample surface may react with V_{Zn}, resulting in the formation of an immobile di-vacancy complex (V_OV_{Zn}) acting as the observed trap and thus explain both the Li and D concentration profiles as observed by SIMS and the presence of open volume defects larger than the isolated V_{Zn} as observed by PAS. In contrast, heat treatment in air will not introduce V_O or any other trap for V_{Zn}, thus even though both Li and V_{Zn} will be mobile under these conditions V_{Zn} will be distributed homogeneously and as the sample is cooled down no redistribution will be observed.

In figure 4 the W- and S-parameters are shown for the V_{Zn}, together with different configurations of the $V_{Zn}V_O$ cluster with and without Li, as obtained by DFT-calculations. Interestingly, it is predicted that $V_{Zn}V_O$ complexes trap positrons and shift the annihilation parameters to higher S-values (to the right in the S-W-plot) as compared to the isolated V_{Zn}, due to the removal of O 2p electrons with the introduction of V_O.

By comparing figure 3 with figure 4 one can observe that several of the calculated defect clusters may correspond to the W- and S-parameter observed for the open volume defect in the hydrogenated sample. However, the observed defect clearly shows an increase in the S-parameter compared to the isolated V_{Zn}. As discussed in the recent paper by Makkonen et al. [17], the addition of V_O to the complex results in an increased S parameter, while the addition of V_{Zn} primarily results in a reduction of the W-parameter. The addition of Li on the Zn-site reduces the open volume of the defect and results in the W- and S-parameters to shift closer to the bulk values, but still positioned above and to the right of the V_{Zn}-line. Furthermore, from figure 4 it is shown that a combination of both H and Li residing on the, O- and Zn-site, respectively, result in annihilation parameters positioned exactly on the Zn-vacancy line, excluding this option. Equal numbers of V_{Zn} and V_O is expected to result in a neutrally charged defect. Increasing the number of V_O will render the defect positively charged, thereby reducing the trapping rate for positrons. Thus the fraction between V_O and V_{Zn} in the observed defect must be limited. Furthermore, a neutral $V_{Zn}V_O$ would fit with the notion in Ref. 10 that the observed defects are weaker positron traps as compared to charged acceptor states, e.g., N_O and Li_{Zn}. From the positron data it is not possible to distinguish between vacancy complexes with or without D or Li, however, SIMS-data (Fig.1) support that at least a fraction of the complexes observed in sample D700 also contain D or Li.

IV. CONCLUSION

The exposure of ZnO to D_2-gas at elevated temperatures have lead to accumulation of D and Li peaking at about 100 nm in depth accompanied with a reduction in the bulk concentration of Li. Positron annihilation spectroscopy show the presence of open volume defects with larger open volume than the isolated Zn-vacancy.

DFT calculations of the annihilation parameters of a range of defect complexes indicates that the formation of a $V_O V_{Zn}$-complex possibly filled by D and/or Li is responsible for the observed accumulation of D and Li. The presence of vacancy complexes close to the surface may strongly affect, e.g., the electrical properties of ZnO and would explain the lack of observation of isolated V_O in samples treated in reducing or Zn-rich samples.

ACKNOWLEDGMENTS

The authors would like to acknowledge the Research Council of Norway for funding of the DYNAZOx-project, (no. 221992) and the Norwegian Micro- and Nano-Fabrication Facility (NorFab 197411/V30). I.M. acknowledges the financial support by the Academy of Finland (Projects No. 285809 and 293932). We acknowledge the computational resources provided by the Aalto Science-IT project and by CSC – the Finnish IT Center for Science.

[1] A. Janotti and C. G. Van de Walle, Physical Review B **76**, 165202 (2007).
[2] T. S. Bjørheim, S. Erdal, K. M. Johansen, K. E. Knutsen, and T. Norby, J. Phys. Chem. C **116**, 23764 (2012).
[3] K. E. Knutsen, A. Galeckas, A. Zubiaga, F. Tuomisto, G. C. Farlow, B. G. Svensson, and A. Y. Kuznetsov, Physical Review B **86**, 121203 (2012).
[4] J. M. Smith and W. E. Vehse, Physics Letters A **31**, 147 (1970).
[5] J. Stehr, K. Johansen, T. Bjrheim, L. Vines, B. Svensson, W. Chen, and I. Buyanova, Physical Review Applied **2**, 021001 (2014).
[6] L. S. Vlasenko and G. D. Watkins, Physical Review B **71**, 125210 (2005).
[7] L. A. Kappers, O. R. Gilliam, S. M. Evans, L. E. Halliburton, and N. C. Giles, Nuclear Instruments and Methods in Physics Research Section B: Beam Interactions with Materials and Atoms **266**, 2953 (2008).
[8] F. Tuomisto, V. Ranki, K. Saarinen, and D. C. Look, Physical Review Letters **91**, 205502 (2003).
[9] F. Tuomisto and I. Makkonen, Reviews of Modern Physics **85**, 1583 (2013).
[10] T. M. Børseth, F. Tuomisto, J. S. Christensen, E. V. Monakhov, B. G. Svensson, and A. Y. Kuznetsov, Physical Review B **77**, 045204 (2008).
[11] A. Zubiaga, F. Tuomisto, V. A. Coleman, H. H. Tan, C. Jagadish, K. Koike, S. Sasa, M. Inoue, and M. Yano, Phys. Rev. B **78**, 035125 (2008).
[12] F. Tuomisto, C. Rauch, M. R. Wagner, A. Hoffmann, S. Eisermann, B. K. Meyer, L. Kilanski, M. C. Tarun, and M. D. McCluskey, Journal of Materials Research **28**, 1977 (2013).
[13] Z. Q. Chen, A. Kawasuso, Y. Xu, H. Naramoto, X. L. Yuan, T. Sekiguchi, R. Suzuki, and T. Ohdaira, Physical Review B **71**, 115213 (2005).
[14] Z. Q. Chen, M. Maekawa, S. Yamamoto, A. Kawasuso, X. L. Yuan, T. Sekiguchi, R. Suzuki, and T. Ohdaira, Physical Review B **69**, 035210 (2004).
[15] K. S. Chan, C. Ton-That, L. Vines, S. Choi, M. R. Phillips, B. G. Svensson, C. Jagadish, and J. Wong-Leung, Journal of Physics D: Applied Physics **47**, 342001 (2014).
[16] M. S. Holston, E. M. Golden, B. E. Kananen, J. W. McClory, N. C. Giles, and L. E. Halliburton, Journal of Applied Physics **119**, 145701 (2016), ISSN 0021-8979, 1089-7550.
[17] I. Makkonen, E. Korhonen, V. Prozheeva, and F. Tuomisto, Journal of Physics: Condensed Matter **28**, 224002 (2016).
[18] F. A. Selim, M. H. Weber, D. Solodovnikov, and K. G. Lynn, Physical Review Letters **99**, 085502 (2007).
[19] E. Boroński and R. M. Nieminen, Phys. Rev. B **34**, 3820 (1986).
[20] G. Kresse and J. Furthmüller, Phys. Rev. B **54**, 11169 (1996).
[21] G. Kresse and D. Joubert, Phys. Rev. B **59**, 1758 (1999).
[22] M. Rummukainen, I. Makkonen, V. Ranki, M. J. Puska, K. Saarinen, and H.-J. L. Gossmann, Phys. Rev. Lett. **94**, 165501 (2005).
[23] S. Hautakangas, I. Makkonen, V. Ranki, M. J. Puska, K. Saarinen, X. Xu, and D. C. Look, Phys. Rev. B **73**, 193301 (2006).
[24] I. Makkonen, A. Snicker, M. J. Puska, J.-M. Mäki, and F. Tuomisto, Phys. Rev. B **82**, 041307 (2010).
[25] I. Makkonen, M. Hakala, and M. J. Puska, Physical Review B **73**, 035103 (2006).
[26] F. Tuomisto, K. Saarinen, D. C. Look, and G. C. Farlow, Physical Review B **72**, 085206 (2005).
[27] A. Zubiaga, F. Tuomisto, V. Coleman, and C. Jagadish, Applied Surface Science **255**, 234 (2008).
[28] K. M. Johansen, J. S. Christensen, E. V. Monakhov, A. Y. Kuznetsov, and B. G. Svensson, Applied Physics Letters **93**, 152109 (2008).
[29] K. M. Johansen, J. S. Christensen, E. V. Monakhov, A. Y. Kuznetsov, and B. G. Svensson, in *Mater. Res. Soc. Symp. Proc.* (Materials Reasearch Society, 2008), vol. 1035, pp. L03–10.
[30] C. G. Van de Walle and J. Neugebauer, Nature **423**, 626 (2003).
[31] K. M. Johansen, H. Haug, E. Lund, E. V. Monakhov, and B. G. Svensson, Applied Physics Letters **97**, 211907 (2010).
[32] K. M. Johansen, A. Zubiaga, F. Tuomisto, E. V. Monakhov, A. Y. Kuznetsov, and B. G. Svensson, Physical Review B **84**, 115203 (2011).
[33] F. Herklotz, A. Hupfer, K. M. Johansen, B. G. Svensson, S. G. Koch, and E. V. Lavrov, Physical Review B **92**, 155203 (2015).
[34] F. Herklotz, K. M. Johansen, A. Galeckas, T. N. Sky, and B. G. Svensson, physica status solidi (b) **253**, 273 (2015).
[35] P. T. Neuvonen, L. Vines, B. G. Svensson, and A. Y. Kuznetsov, Physical Review Letters **110**, 015501 (2013).

[36] A. Y. Azarov, K. E. Knutsen, P. T. Neuvonen, L. Vines, B. G. Svensson, and A. Y. Kuznetsov, Phys. Rev. Lett. **110**, 175503 (2013).
[37] K. M. Johansen, A. Zubiaga, I. Makkonen, F. Tuomisto, P. T. Neuvonen, K. E. Knutsen, E. V. Monakhov, A. Y. Kuznetsov, and B. G. Svensson, Physical Review B **83**, 245208 (2011).
[38] K. J. Fischer, Journal of Crystal Growth **34**, 139 (1976).
[39] A. Janotti and C. G. Van de Walle, Reports on Progress in Physics **72**, 126501 (2009).
[40] A. Carvalho, A. Alkauskas, A. Pasquarello, A. K. Tagantsev, and N. Setter, Physical Review B **80**, 195205 (2009).
[41] K. E. Knutsen, K. M. Johansen, P. T. Neuvonen, B. G. Svensson, and A. Y. Kuznetsov, Journal of Applied Physics **113**, 023702 (2013).
[42] M. D. McCluskey, S. J. Jokela, K. K. Zhuravlev, P. J. Simpson, and K. G. Lynn, Applied Physics Letters **81**, 3807 (2002).
[43] E. V. Lavrov, F. Herklotz, and J. Weber, Physical Review B **79**, 165210 (2009).
[44] E. V. Lavrov, F. Herklotz, and J. Weber, Physical Review Letters **102**, 185502 (2009).
[45] G.-Y. Huang, C.-Y. Wang, and J.-T. Wang, Solid State Communications **149**, 199 (2009).
[46] B. Puchala and D. Morgan, Physical Review B **85**, 064106 (2012).